A haploid mammalian genetic screen identifies UBXD8 as a key determinant of HMGCR degradation and cholesterol biosynthesis

Anke Loregger[1], Matthijs Raaben[2], Josephine Tan[1], Saskia Scheij[1], Martina Moeton[1], Marlene van den Berg[1], Hila Gelberg-Etel[5,6], Elmer Stickel[2], Joseph Roitelman[5,6], Thijn Brummelkamp[2,3,4], Noam Zelcer[1,7]

Supplementary information

Itemized list of supplementary information

1) ***Supplementary figure I***: Characterization of Hap1-HMGCR-mNeon cells
2) ***Supplementary figure II***: HMGCR-mNeon is subject to sterol-stimulated degradation
3) ***Supplementary figure III***: Integration sites in a subset of trapped genes
4) ***Supplementary figure IV***: Pathway analysis of trapped genes in HMGCR-mNeonHIGH cells
5) ***Supplementary figure V***: Time-dependent sterol-stimulated degradation of HMGCR-mNeon in Hap1 cells
6) ***Supplementary figure VI***: Quantification of immunoblots shown in Figure 3A-D
7) ***Supplementary figure VII***: UBXD8 is required for sterol-stimulated degradation of HMGCR in human- and murine-derived hepatocytes
8) ***Supplementary figure VIII***: Time-dependent degradation of HMGCR-mNeon in UBXD8KO cells
9) ***Supplementary figure IX***: Sterol-dependent ubiquitylation of HMGCR is intact in UBXD8KO cells
10) ***Supplementary figure X:*** UBXD8 governs cholesterol synthesis in hepatocytes
11) ***Supplementary table I***: Sequence of the CRIS-PITCh mNeon-2A-PURO cassette targeting HMGCR
12) ***Supplementary table II***: Oligonucleotide sequences
13) ***Supplementary table III***: Identified genes in HMGCR-mNeon screen
14) ***Supplementary movie I***: HMGCR-mNeon degradation in live cells

Supplementary figure legends

Supplementary Figure I Characterization of Hap1-HMGCR-mNeon cells. (***A***) Genomic sequences from 4 independent clones covering the targeted 5' and 3' integration sites were determined. The target genomic sequence is shown at the top and nucleotides in red indicate the microhomology domains. Nucleotides in italics indicate insertions (***B***) The indicated Hap1-HMGCR-mNeon clones were cultured in sterol-containing- or sterol-depletion medium for 24 hrs. Subsequently, mNeon intensity in cells was determined by FACS analysis. (***C***) Cells were grown on glass coverslips and cultured in sterol-depletion medium for 24 hrs to induce expression of *HMGCR-mNeon*. Subsequently, cells were fixed and stained as indicated. Scale bar: 10 μm (***D***) HepG2 cells were cultured in sterol-containing- or sterol-depletion medium for 24 hrs. Subsequently, cells were treated with 10 μM 25-HC and 25 μM MG132 for 2 hrs as shown. Total cell lysates were immunoblotted as indicated and immunoblot is representative of three independent experiments.

Supplementary Figure II. HMGCR-mNeon is subject to sterol-stimulated degradation. (***A***) The indicated Hap1-HMGCR-mNeon clones were cultured in sterol-containing- or sterol-depletion medium for 24 hrs. Subsequently, cells were treated with 10 μM 25-HC for 1 hr after which mNeon intensity was determined by FACS analysis. (***B***) Hap1-HMGCR-mNeon cells were cultured in sterol-depletion medium for 22 hrs. Cells were then treated with 10 μM 25-HC for an additional 3 hrs and images of live cells were taken at 20 min intervals (movie S1). Images acquired at the indicated time points are shown.

Supplementary Figure III. Integration sites in a subset of trapped genes. The disruptive integration sites in the $mNeon^{HIGH}$ and $mNeon^{LOW}$ populations within the indicated genes are shown mapped to the corresponding genomic loci.

Supplementary Figure IV. Pathway analysis of trapped genes in HMGCR-$mNeon^{HIGH}$ cells. The set of significant ($p<0.05$) genes identified in HMGCR-$mNeon^{HIGH}$ cells were analyzed using Metascape (http://metascape.org). The top 20 GO biological processes that were enriched are shown.

Supplementary Figure V. Time-dependent sterol-stimulated degradation of HMGCR-mNeon in Hap1 cells. Control and UBXD8KO#2 Hap1 cells were cultured in sterol-depletion medium for 24 hrs and then treated with 10 μM 25-HC for the indicated time. Total cell lysates were immunoblotted as indicated, and immunoblot is representative of three independent experiments. Numbers represent the mean HMGCR-mNeon intensity of three independent experiments.

Supplementary Figure VI. Quantification of immunoblots shown in Figure 3A-D. The intensity of HMGCR was normalized to that of ACTIN and each bar and error are the mean ± SEM of at least n=3.

Supplementary Figure VII. UBXD8 is required for sterol-stimulated degradation of

HMGCR in human- and murine-derived hepatocytes. (***A,B***) IHH and (***C***) Hepa1-6 control and the indicated UBXD8KO clones were cultured in sterol-containing- or sterol-depletion medium for 24 hrs, after which (***A,C***) cells were treated with 10 μM 25-HC for the indicated time. Total cell lysates were immunoblotted as indicated, and immunoblot is representative of three independent experiments. (***B***) IHH control and two independent UBXD8KO clones were cultured as in ***A*** and mRNA expression of the indicated genes was determined by qPCR. Each bar and error represent the mean ± SD (n=3).

Supplementary Figure VIII. Time-dependent degradation of HMGCR-mNeon in UBXD8KO cells. Control (Ctrl), or Hap1-UBXD8KO cells in which the full length (FL) or the indicated UBXD8 variants were stably reintroduced were cultured in sterol-depletion medium for 24 hrs and then treated with 10 μM 25-HC for the indicated time after which the intensity of mNeon fluorescence was quantified by FACS analysis (n=3).

Supplementary Figure IX. Sterol-dependent ubiquitylation of HMGCR is intact in UBXD8KO cells. HepG2 UBXD8KO cells were cultured in sterol-depletion medium for 24 hrs and then treated with 10 μM 25-HC for 2 hours. Subsequently, HMGCR was immunoprecipitated from total cell lysates and immunoblotted as indicated. Immunoblot is representative of 3 independent experiments.

Supplementary Figure X. UBXD8 governs cholesterol synthesis in hepatocytes. (***A***) HepG2 control and UBXD8KO #1 were sterol-depleted by culture in β-MCD-containing medium for 16 hrs. Subsequently, cells were labeled for 2 hours with [^{14}C]-pyruvate in the presence of 10 μM 25-HC or 2.5 μg/mL simvastatin, as indicated. The [^{14}C]-labeled non-saponifiable lipid fraction, extracted from samples containing an equal amount of cellular protein, was quantified by scintillation counting. Each bar and error are the mean ± SD of percent HMGCR activity (n=4); ** $p < 0.01$, *** $p < 0.001$.

Supplementary Movie I. Live cell imaging of Hap1-HMGCR-mNeon cells. Hap1-HMGCR-mNeon cells were cultured in sterol-depletion medium for 22 hrs. Subsequently, cells were treated with 10 μM 25-HC for up to 4 hrs, as schematically depicted in Fig. S2B. Images were taken at 20 min intervals throughout the entire experiment.

Supplementary Table I. Sequence of the CRIS-PITCh mNeon-2A-PURO cassette targeting *HMGCR*. The sequence of the mNeon-2A-PURO cassette was cloned into pGEM-T and used to target the last exon of *HMGCR* as shown in Figure 1A. Microhomology domains are highlighted in bold. Target sites for CRISPR/Cas9 are underlined. Green-, red- and blue-colored nucleotides indicate the coding sequences of mNeon, 2A peptide, and the puromycin resistance gene, respectively. Proper targeting requires an sgRNAs that targets the last exon of *HMGCR*, and two sgRNAs that target the underlined microhomology region to release the donor fragment.

Supplementary Table II. Oligonucleotide sequences. The sequence of the sgRNA-encoding oligonucleotides used in this study is indicated. Oligonucleotides were annealed and ligated into the *BbsI* site in px330.

Supplementary Table III. Identified genes in HMGCR-mNeon screen. Detailed table listing the gene-based insertions identified in the HMGCR-mNeon screen.

A haploid mammalian genetic screen identifies UBXD8 as a key determinant of HMGCR degradation and cholesterol biosynthesis

Anke Loregger[1], Matthijs Raaben[2], Josephine Tan[1], Saskia Scheij[1], Martina Moeton[1], Marlene van den Berg[1], Hila Gelberg-Etel[3], Elmer Stickel[2], Joseph Roitelman[5], Thijn Brummelkamp[2,3,4], Noam Zelcer[1,6]

Supplementary information

Supplementary Figure I

A

5' Junction			3' Junction		
	TACAAGACCTCCAAGGACGGATCCATGGTGAG			GCCTGAAGCTTGCACCAAGAAGACAGCCTGA	
#1	TACAAGACCTCCAAGG*CTCCAAGG*ACGGATCCATGGTGAG	+8	#1	GCCTGAAGCTTGCA*AGCTTGA*ACCAAGAAGACAGCCTGA	+8
#2	TACAAGACCTCCAAGG*ATCCAAGG*ACGGATCCATGGTGAG	+8	#2	GCCTGAAGCTTGCA*AGCTTGA*ACCAAGAAGACAGCCTGA	+8
#3	TACAAGACCTCCAAGG*CAAGG*ACGGATCCATGGTGAG	+5	#3	GCCTG-*AGCTTGCA*CCAAGAAGACAGCCTGA	-1
#4	TACAAGACCTCCAAGG*CTCCAAGG*ACGGATCCATGGTGAG	+8	#4	GCCTGAAGCTTGCA*AGCTTGA*ACCAAGAAGACAGCCTGA	+8

B

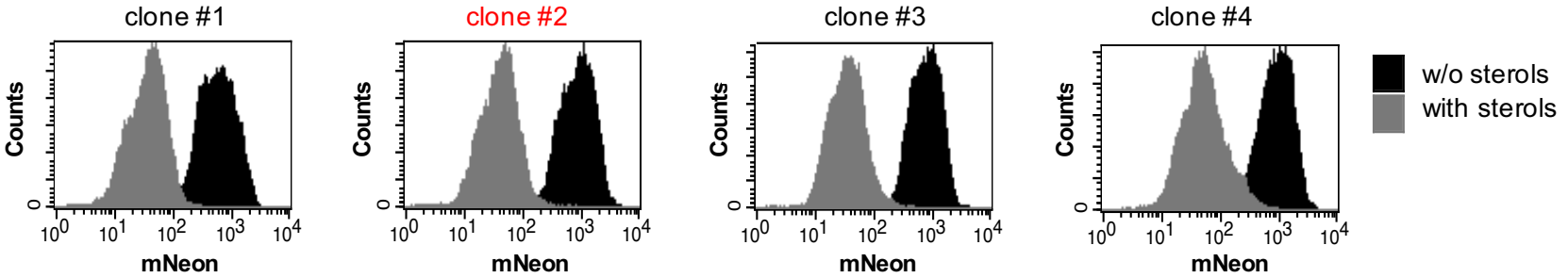

C

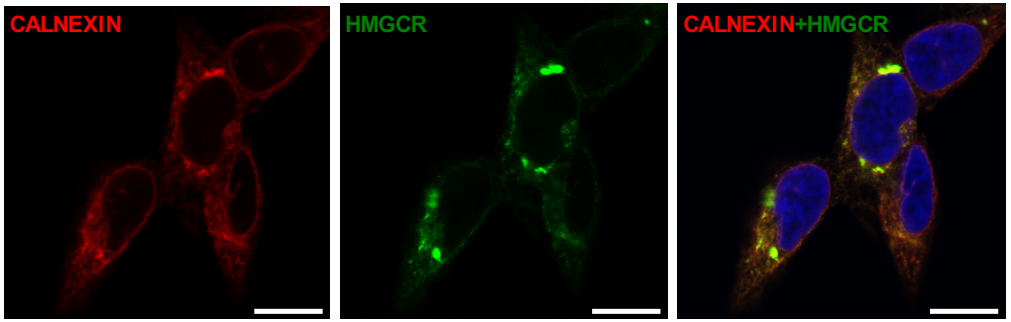

D

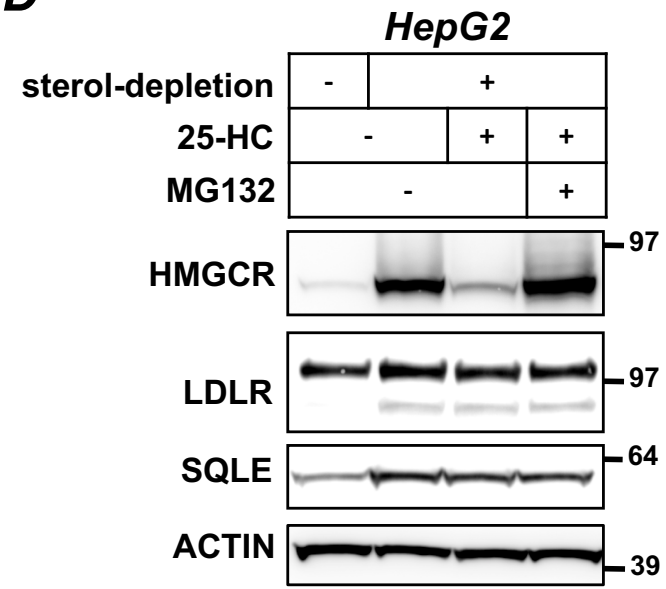

Supplementary Figure II

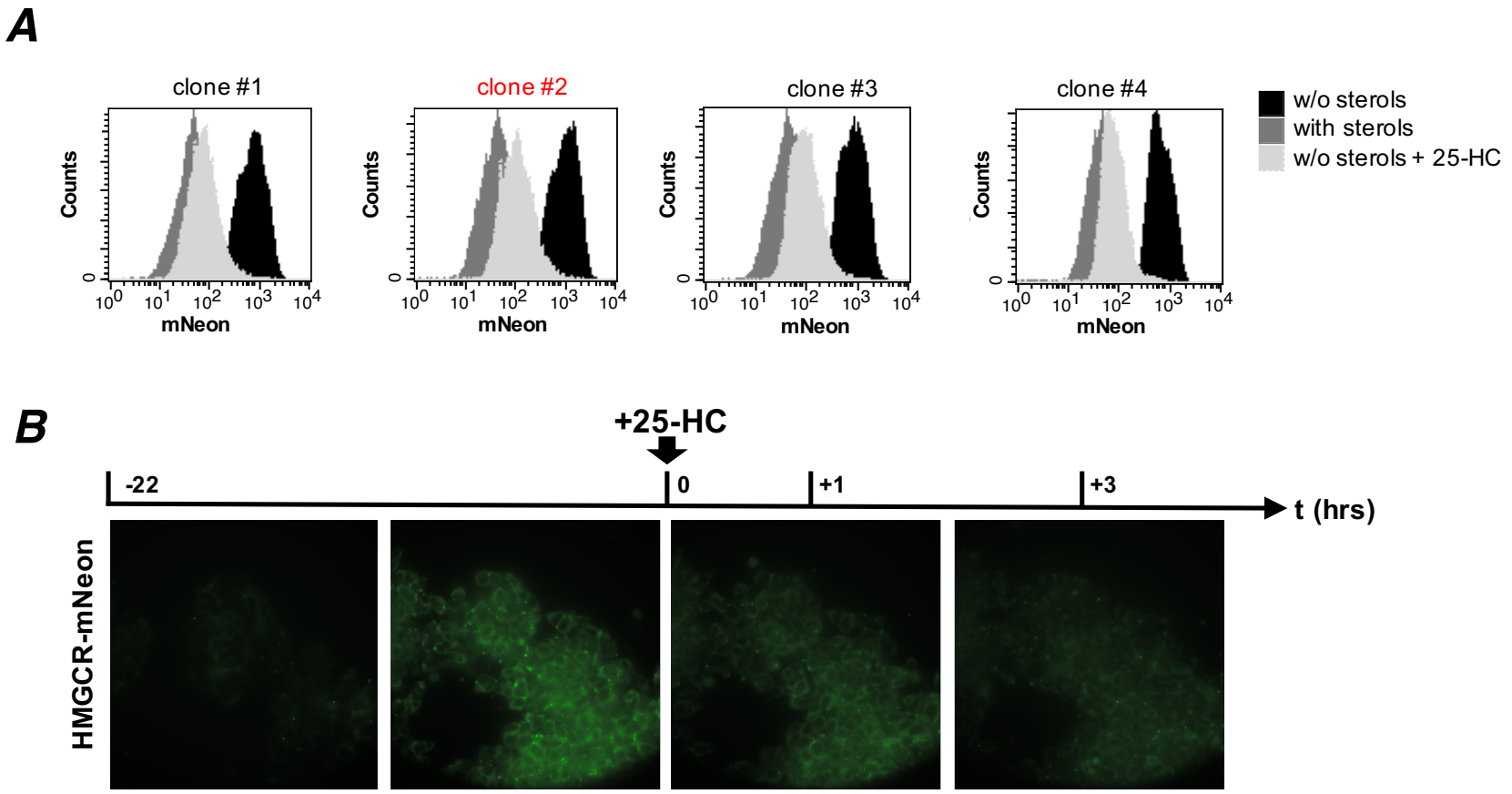

Supplementary Figure III

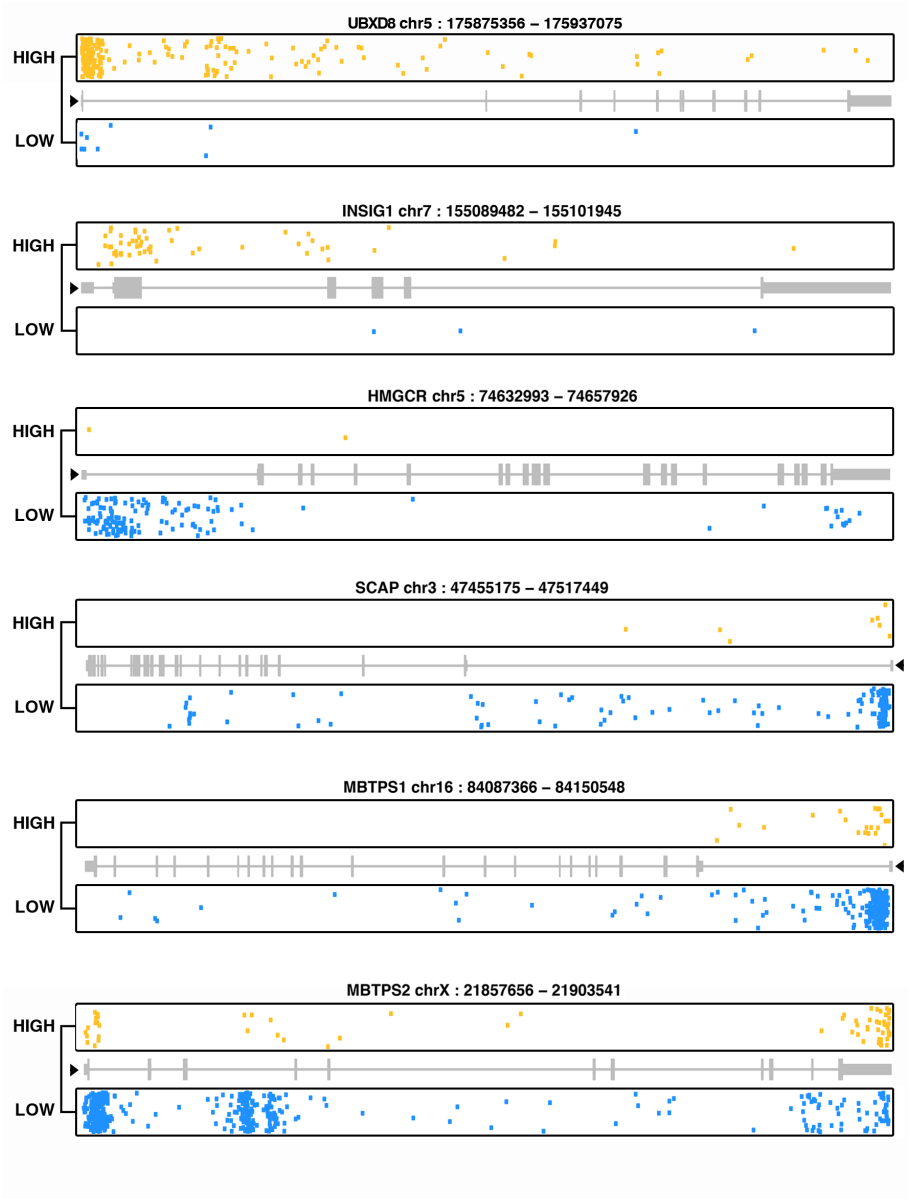

Supplementary Figure IV

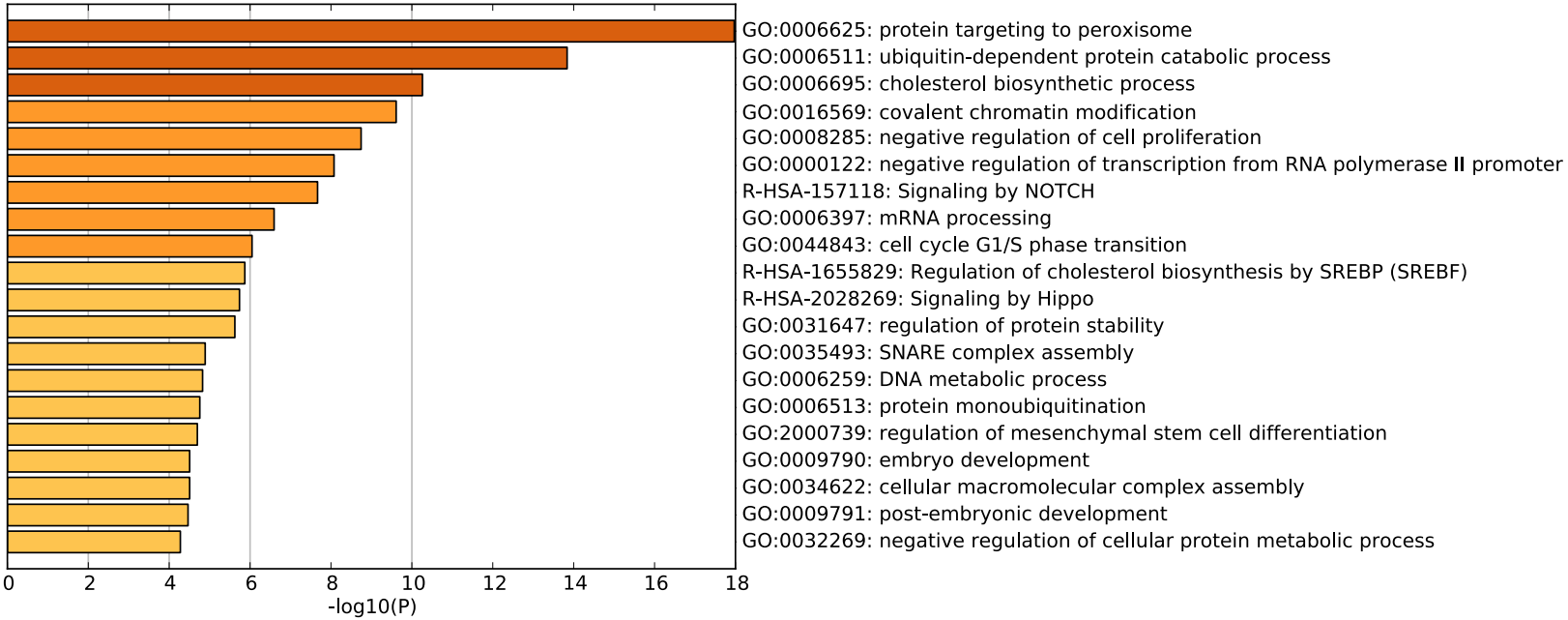

Supplementary Figure V

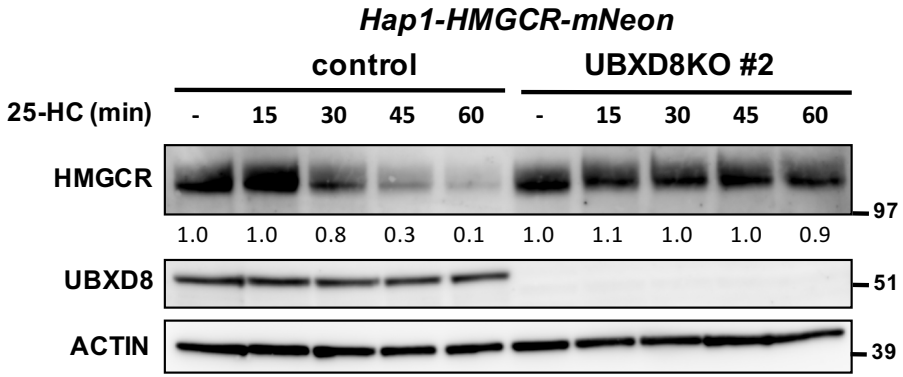

Supplementary Figure VI

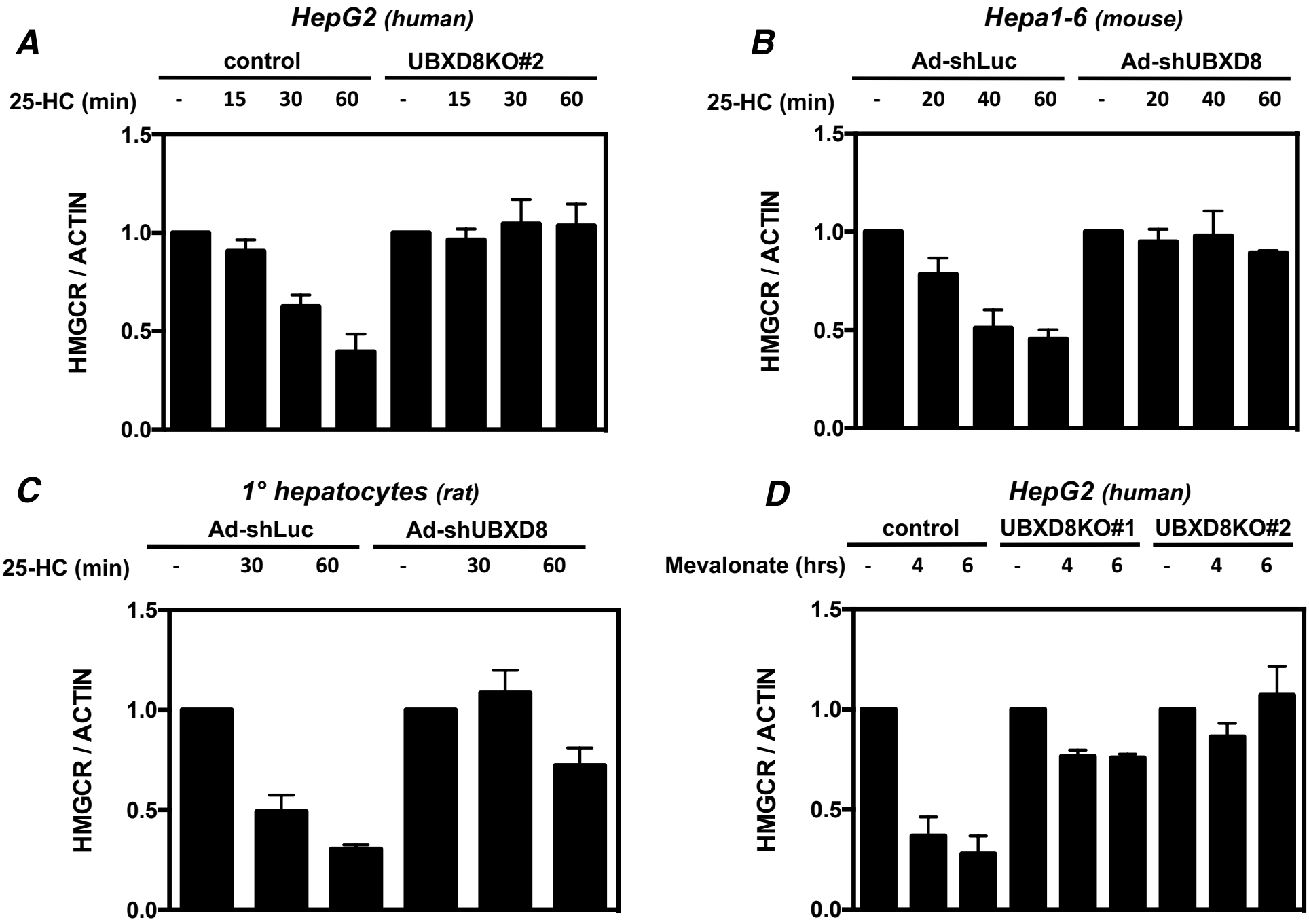

Supplementary Figure VII

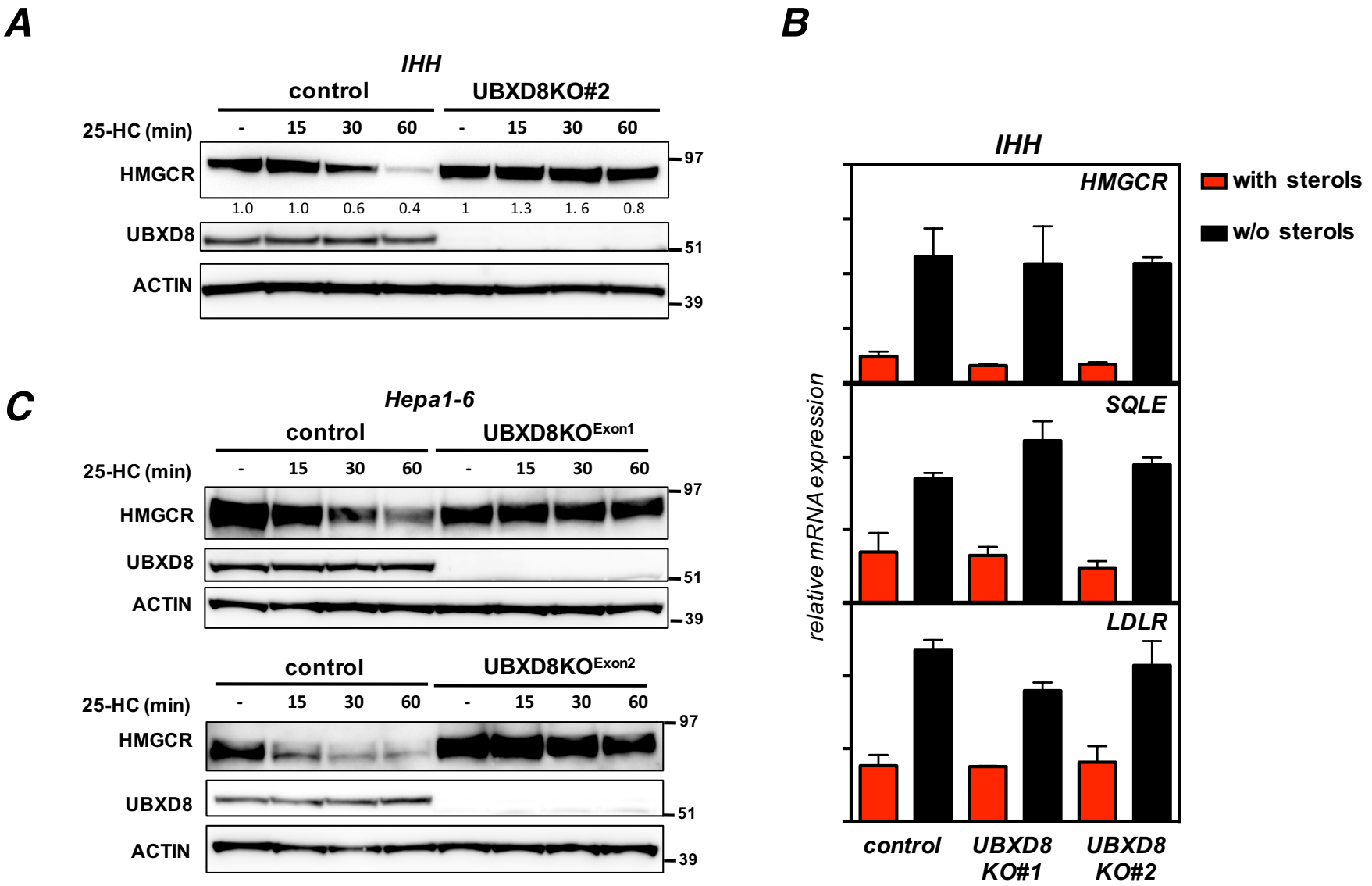

Supplementary Figure VIII

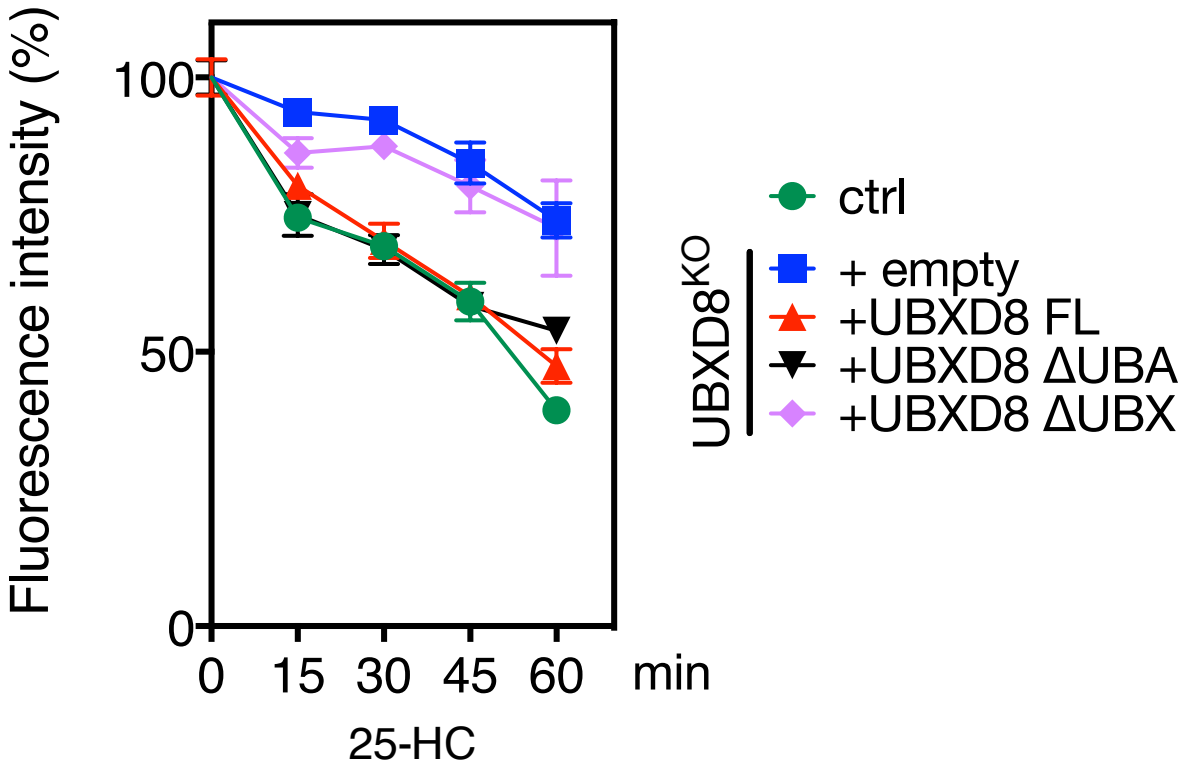

Supplementary Figure IX

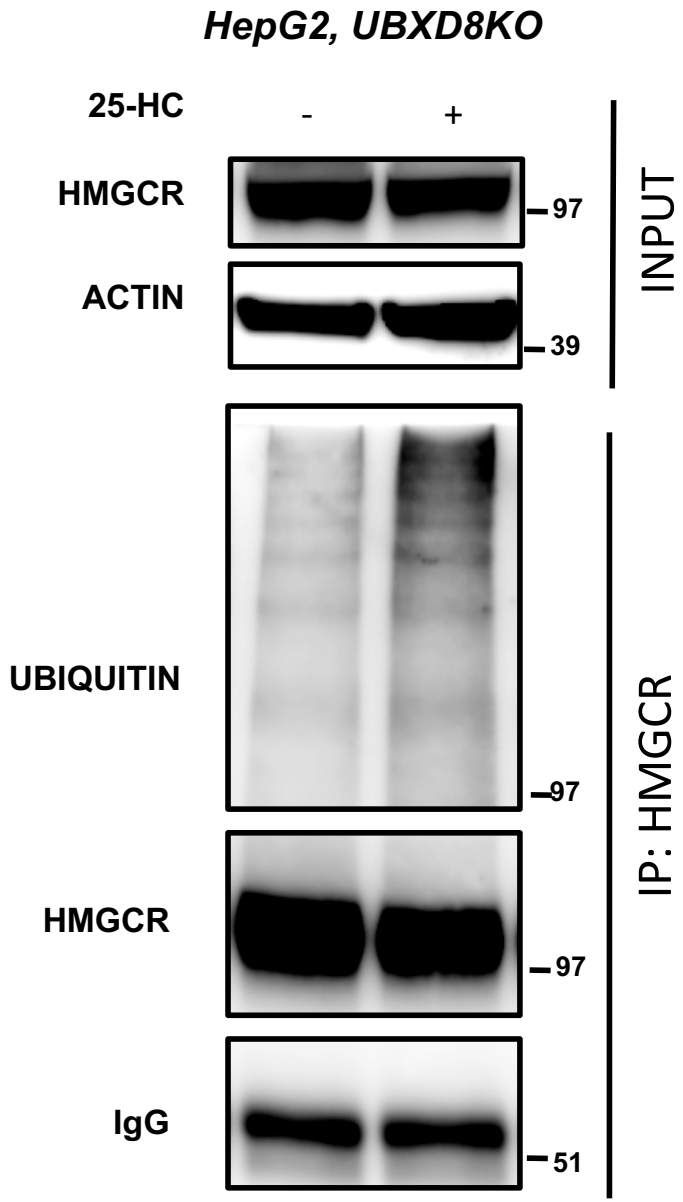

Supplementary Figure X